Structural and Functional Properties of Deep Abdominal Subcutaneous Adipose Tissue Explain Its Association With Insulin Resistance and Cardiovascular Risk in Men

Kyriakoula Marinou,[1,2] Leanne Hodson,[1] Senthil K. Vasan,[1,3] Barbara A. Fielding,[1,4] Rajarshi Banerjee,[5] Kerstin Brismar,[3] Michael Koutsilieris,[2] Anne Clark,[1] Matt J. Neville,[1,6] and Fredrik Karpe[1,6]

OBJECTIVE

Fat distribution is an important variable explaining metabolic heterogeneity of obesity. Abdominal subcutaneous adipose tissue (SAT) is divided by the Scarpa's fascia into a deep subcutaneous adipose tissue (dSAT) and a superficial subcutaneous adipose tissue (sSAT) layer. This study sought to characterize functional differences between the two SAT layers to explore their relative contribution to metabolic traits and cardiovascular risk (CVR) profile.

RESEARCH DESIGN AND METHODS

We recruited 371 Caucasians consecutively from a local random, population-based screening project in Oxford and 25 Asian Indians from the local community. The depth of the SAT layers was determined by ultrasound (US), and adipose tissue (AT) biopsies were performed under US guidance in a subgroup of 43 Caucasians. Visceral adipose tissue (VAT) mass was quantified by dual-energy X-ray absorptiometry scan.

RESULTS

Male adiposity in both ethnic groups was characterized by a disproportionate expansion of dSAT, which was strongly correlated with VAT mass. dSAT depth was a strong predictor of global insulin resistance (IR; homeostatic model assessment of IR), liver-specific IR (insulin-like growth factor binding protein-1), and Framingham risk score independently of other measures of adiposity in men. Moreover, dSAT had higher expression of proinflammatory, lipogenic, and lipolytic genes and contained higher proportions of saturated fatty acids. There was increased proportion of small adipocytes in dSAT.

CONCLUSIONS

SAT is heterogeneous; dSAT expands disproportionally more than sSAT with increasing obesity in Caucasian males (confirmed also in Asian Indians). Its expansion is related to increased CVR independent of other adiposity measures, and it has biological properties suggestive of higher metabolic activity contributing to global IR.

Diabetes Care 2014;37:821–829 | DOI: 10.2337/dc13-1353

[1]Oxford Centre for Diabetes, Endocrinology, and Metabolism, Radcliffe Department of Medicine, University of Oxford, Oxford, United Kingdom
[2]Department of Experimental Physiology, Athens University School of Medicine, Athens, Greece
[3]Department of Molecular Medicine and Surgery, Karolinska Institutet, Stockholm, Sweden
[4]Faculty of Health and Medical Sciences, University of Surrey, Guildford, United Kingdom
[5]Division of Cardiovascular Medicine, Radcliffe Department of Medicine, University of Oxford, Oxford, United Kingdom
[6]National Institute for Health Research, Oxford Biomedical Research Centre, Oxford University Hospital Trusts, Oxford, United Kingdom

Corresponding author: Fredrik Karpe, fredrik.karpe@ocdem.ox.ac.uk.

Received 6 June 2013 and accepted 21 October 2013.

This article contains Supplementary Data online at http://care.diabetesjournals.org/lookup/suppl/doi:10.2337/dc13-1353/-/DC1.

The contents of this article reflect only the authors' views and not the views of the European Commission.

Abdominal obesity is associated with the development of insulin resistance (IR), type 2 diabetes, and coronary heart disease (1). The classical abdominal adipose tissue (AT) compartmentalization into subcutaneous adipose tissue (SAT) and visceral adipose tissue (VAT) has been widely studied in relation to obesity-related complications (2–4). The anatomical distinction of SAT compartments into superficial subcutaneous adipose tissue (sSAT) and deep subcutaneous adipose tissue (dSAT), divided by Scarpa's fascia, is well documented in literature (5–9). A few studies have shown that dSAT is strongly related to IR in a manner nearly identical to that of VAT, while sSAT follows the pattern of lower-body SAT (1,10). Of note, Golan et al. (11) recently demonstrated that sSAT was a protective fat depot in patients with type 2 diabetes.

The sSAT layer is organized in compact fascial septa orientated perpendicular to the skin, with the lobules being small and ovoid, whereas the dSAT layer contains larger lobules and less organized and widely spaced Scarpa's fascia septa (5,12–14). Studies in pigs suggest that the SAT layers have different embryological origin and that the deeper layer expands during weight gain (1,15). The situation in humans is less clear.

Importantly, fat distribution differs between males and females, and this has been related to differences in both cardiovascular and diabetes risk profile between genders (3,16–18).

The current cross-sectional study was undertaken with three primary objectives: *1*) to identify the depth of the different SAT layers by a novel and simple technique using ultrasound (US) imaging, validated against magnetic resonance imaging (MRI) and dual-energy X-ray absorptiometry (DEXA) in healthy volunteers within a wide variety of adiposity; *2*) to confirm the differences between sSAT and dSAT and their relation with metabolic markers associated with IR and cardiometabolic risk; and *3*) to characterize the biological differences between sSAT and dSAT by evaluating whether there are structural differences in the SAT layers, gene expression, and fatty acid (FA) profiles. We hypothesized that dSAT is morphologically and biologically different than sSAT, with the deep layer having a more proinflammatory, lipogenic, and lipolytic profile. We also hypothesized that the relative expansion of dSAT against sSAT layer, as quantified by US, may be a more superior index than BMI and waist circumference (WC) to characterize cardiovascular and diabetes risk.

RESEARCH DESIGN AND METHODS

Clinical Protocol

The study participants were enrolled consecutively from a random and population-based screening project of Caucasian residents in Oxfordshire, the Oxford Biobank (www.oxfordbiobank.org.uk) (19). Because of the well-known high diabetes risk and the tendency toward IR, we also included a pilot recruitment of 25 nondiabetic Asian Indian immigrants to the U.K. from the local Asian Oxfordshire community (as described below). Then, from the main Oxford Biobank study cohort, we identified 25 Caucasians with identical whole subcutaneous adipose tissue (wSAT), age, and gender with the recruited Asians (nested study).

Caucasian Cohort

The 371 Caucasian individuals (146 men, 225 women) came to the clinical research unit after an overnight fast. Anthropometric variables were measured, blood samples were taken, and US measurements of the abdomen were made. The distribution of cardiovascular risk (CVR) was estimated by calculating the Framingham risk score (FRS). The Framingham calculations of 10-year CVR were based on the third report of the National Cholesterol Education Program Expert Panel on Detection, Evaluation, and Treatment of High Blood Cholesterol in Adults (Adult Treatment Panel III) (2). The study population did not include any patient with prior diagnosis of coronary heart disease. AT biopsies were specifically taken from sSAT and dSAT layers in a subset (n = 43) of the Caucasian individuals.

Asian Indians

The 25 Asian Indian individuals attended the clinical research unit for US characterization of sSAT and dSAT. The study population recruitment algorithm is presented in Supplementary Fig. 1.

Study Primary End Points

The primary end points of the study were *1*) the measurement of the depth of dSAT and sSAT layers by US (linked with all the other study end points), *2*) gene expression and FA profile of dSAT and sSAT, *3*) circulating lipid profile and IR, and *4*) histological characteristics of dSAT and sSAT.

Study Secondary End Points

The secondary end points of the study were *1*) measurement of dSAT and sSAT by MRI (as means to validate the US measurements), *2*) DEXA measurements of abdominal obesity, *3*) FRS, and *4*) circulating biomarkers.

The study was approved by the Oxfordshire Clinical Research Ethics Committee, and all volunteers gave written informed consent.

Ultrasonography of SAT

US measurements of the SAT layers were performed using a 7.5 MHz linear array probe and two-dimensional imaging (Philips PDI 5000) in all participants (n = 371). Measurements were taken with participants in the supine position during exhalation phase. All measurements were recorded 5 cm lateral to the umbilicus (a location where the Scarpa's fascia line is clearly observed) on both sides. The probe was held with 1–2 mm distance from the skin (US gel layer giving contact) to ensure no pressure was put on the abdomen. Two independent measurements were recorded from each side, and the final depth of the fat depots was obtained by the average of all four measurements. The sSAT distance was defined as the region of AT between the Scarpa's fascia and lower dermis, whereas wSAT was defined as the AT occupying the space between the anterior line of the rectus abdominis muscle and lower dermis. The difference between wSAT and sSAT was defined as dSAT. To evaluate the within-person measurement variability, four measurements taken 10 min apart were recorded in 24 subjects (12 males, 12 females), and the intraobserver variability was 0.18% for sSAT, 0.3% for dSAT, and 0.06% for wSAT. The intraclass correlation coefficient was

0.99 for wSAT ($P < 0.0001$), 0.98 for dSAT ($P < 0.0001$), and 0.98 for sSAT ($P < 0.0001$).

MRI

SAT measured by US was validated using single-slice MRI in 18 Caucasian women. A transverse turbo spin echo image of the abdomen was acquired at the L4 level in a 3 Tesla MRI scanner (Siemens Tim Trio; Siemens Medical Solutions, Erlangen, Germany). The depth of sSAT and dSAT layers were measured at 5 cm either side of the midline, with the skin excluded.

DEXA scan

A total of 225 Caucasian participants with US measurements underwent DEXA scanning (GE Health Care Lunar iDexa, software version 14.1) for quantification of VAT and trunk/android fat mass. The algorithm of the software provides estimates of VAT mass with high accuracy (20).

Biochemical Analyses

Biochemical analyses were performed in all 371 of the Caucasian individuals. Plasma glucose, triglycerides (TG), nonesterified FAs, high-sensitivity C-reactive protein, total cholesterol, LDL cholesterol, HDL cholesterol, apolipoprotein B, apolipoprotein A1 were determined enzymatically using an ILAB 650 Multianalyzer (Instrumentation Laboratory, Warrington, U.K.). Plasma insulin concentrations were analyzed by radioimmunoassay kits (Linco Research St. Charles, MO). IR was estimated using homeostatic model assessment of IR (HOMA-IR) (21). Serum insulin-like growth factor binding protein-1 concentrations were measured as a separate indicator of liver-specific IR (22) and were determined by radioimmunoassay (23). Blood pressure was recorded after 10 min rest by doing three consecutive readings (Omron).

Biopsies

Biopsies were performed in 43 of the Caucasian individuals. SAT biopsies (from dSAT and sSAT on the same occasion) were performed under US guidance. After administration of local anesthesia (5–10 ml of 1% lignocaine), a single entry point was made and AT was first obtained from dSAT using a 12-G aspiration needle, followed by a biopsy of the sSAT using a different syringe and needle. This technique yielded ~300 mg of fat from each layer. Samples were washed with saline and aliquoted in 4% formalin or in RNA-Later solution for RNA extraction.

Gene Expression Studies

The AT biopsy samples were removed from RNA-Later and homogenized in TRIzol reagent (24). The lipid layer was removed and stored for FA analysis (n = 22) (25). Total RNA from AT (n = 43) was isolated using a mirVana microRNA solution kit (Applied Biosystems) as described (24).

The mRNA expressions of adiponectin (*ADIPOQ*), adiponectin receptor-1 (*ADIPOR1*), adiponectin receptor-2 (*ADIPOR2*), leptin (*LEP*), stearoyl-CoA desaturase-1 (*SCD1*), FA synthase (*FASN*), fatty acyl elongase-5 and -6 (*ELOVL5* and *ELOVL6*), peroxisome proliferator-activated receptor γ-2 (*PPARγ2*), interleukin-6 (*IL6*), monocyte chemotactic protein-1 (*MCP1*), Lipoprotein lipase (*LPL*), and hormone-sensitive lipase (*LIPE*) were quantified by real-time PCR using TaqMan gene expression assays (Applied Biosystems) and normalized to the expression of the three previously validated stable endogenous control transcripts: cyclophilin A (*PPIA*), phosphoglycerate kinase 1 (*PGK1*), and importin 8 (*IPO8*) using the $\Delta\Delta C_t$ method (24).

Analysis of AT TG FA composition

A sample of 200 μL of the lipid layer from the RNA isolation step was used to determine TG FA composition as described previously (25). FA composition (μmol/100 μmol total FA) was determined by gas chromatography (26).

Cell Size Analysis

sSAT and dSAT samples were embedded in paraffin and cut in 5 μm sections. Each section was dewaxed and stained with hematoxylin–eosin. The adipocyte size analysis was based on the method of Chen and Fareze (27) using Adobe Photoshop CS2 9.0.2 (Adobe Systems, San Jose, CA) and an image processing tool kit (Reindeer Games, Gainesville, FL). The histological cell sizing was performed by an operator blinded to the origin of the tissue. In order to define the minimum number of cells required for accurate determination of cell size distribution in a sample, we took five samples and counted 2,500 cells in each. We then removed data 100 at a time and observed that the coefficient of variation started to increase when less than 100 cells were included in each biopsy. Therefore we included only biopsies with more than 100 cells available for quantification (n = 23 pairs).

Statistical Analysis

Continuous variables were tested for normal distribution by using Kolmogorov–Smirnov test, and a significance level <0.05 was used to reject the null hypothesis of normal distribution. Skewed samples sets were log transformed prior to statistical analysis to achieve normal distribution. Comparisons of continuous variables between two groups were performed using an unpaired t test, while comparisons between the two SAT layers (within the same persons) were performed using a paired t test. All continuous variables are expressed as means ± SEM unless otherwise stated. For histology studies, cells size distribution between the two SAT layers were compared by using one-way ANOVA followed by paired t tests for individual comparisons. Categorical variables were compared using χ^2 test, as appropriate. Correlations between continuous variables were assessed using bivariate analysis, and Pearson's coefficient was estimated. Z score was calculated in order to compare the Pearson's coefficient. The differences in FRS between groups were compared by using one-way ANOVA.

Linear regression analysis of IR was performed using log HOMA-IR as a dependent variable and log(dSAT) and log(WC) as independent variables, and results are presented as standardized betas (log[BMI] was not included in the models due to colinearity with log[WC]). Linear regression of FRS was performed using FRS as a dependent variable and BMI, dSAT, sSAT, and HOMA IR as independent variables. All statistical tests were performed using SPSS v.20.0 (USA).

RESULTS

Caucasian participant characteristics, including anthropometric variables, blood biochemistry, and measures of IR, are presented in Supplementary Table 1.

SAT Layers Measured Using US Correlate Strongly With SAT Measurements Using MRI

The sSAT, dSAT, and wSAT distances were quantified by US correlated with the SAT measurements by MRI ($r = 0.75$ [$P < 0.0001$] for dSAT, $r = 0.78$ [$P < 0.0001$] for sSAT, and $r = 0.85$ [$P < 0.0001$] for wSAT).

dSAT Distance Estimated by US Is Strongly Correlated With DEXA-Estimated VAT

We observed that android and trunk mass measured by DEXA in 225 Caucasian individuals were positively correlated with wSAT ($r = 0.66$ [$P < 0.0001$] for android, $r = 0.60$ [$P < 0.0001$] for trunk mass). VAT was most strongly correlated with dSAT ($r = 0.73$; $P < 0.0001$) and to a lesser degree with sSAT ($r = 0.44$, $P < 0.0001$; z score 4.632, $P = 0.000004$).

Male Adiposity Is Characterized by a Disproportionate Increase in dSAT

Although men and women had similar wSAT, men had significantly thicker dSAT and thinner sSAT than women (Fig. 1*A*), while VAT was greater in men (Fig. 1*B*). Accordingly, dSAT:wSAT ratio was significantly greater in men than in women (0.60 ± 0.01 vs. 0.48 ± 0.007; $P < 0.0001$). In the study of the South Asian Indian migrants, we hypothesized that the dSAT would be proportionally larger in both men and women. We therefore selected controls with the same wSAT depth and compared the dSAT and sSAT between the ethnic groups. There was no obvious difference ($P = 0.31$ for dSAT, $P = 0.29$ for sSAT).

We then examined the relationships between SAT layers and other anthropometric variables, biochemical characteristics, measures of IR, and blood pressure in men and women separately. The ratio of dSAT:wSAT was correlated with BMI, WC, waist-to-hip ratio, and wSAT (Supplementary Table 2) in men. In women, both dSAT and sSAT were similarly expanded in obesity, and the dSAT:wSAT ratio was only weakly correlated with BMI, WC, waist-to-hip ratio, and wSAT. The correlations between SAT layers and markers of IR, metabolic indices, and CVR profile are presented in Supplementary Table 3.

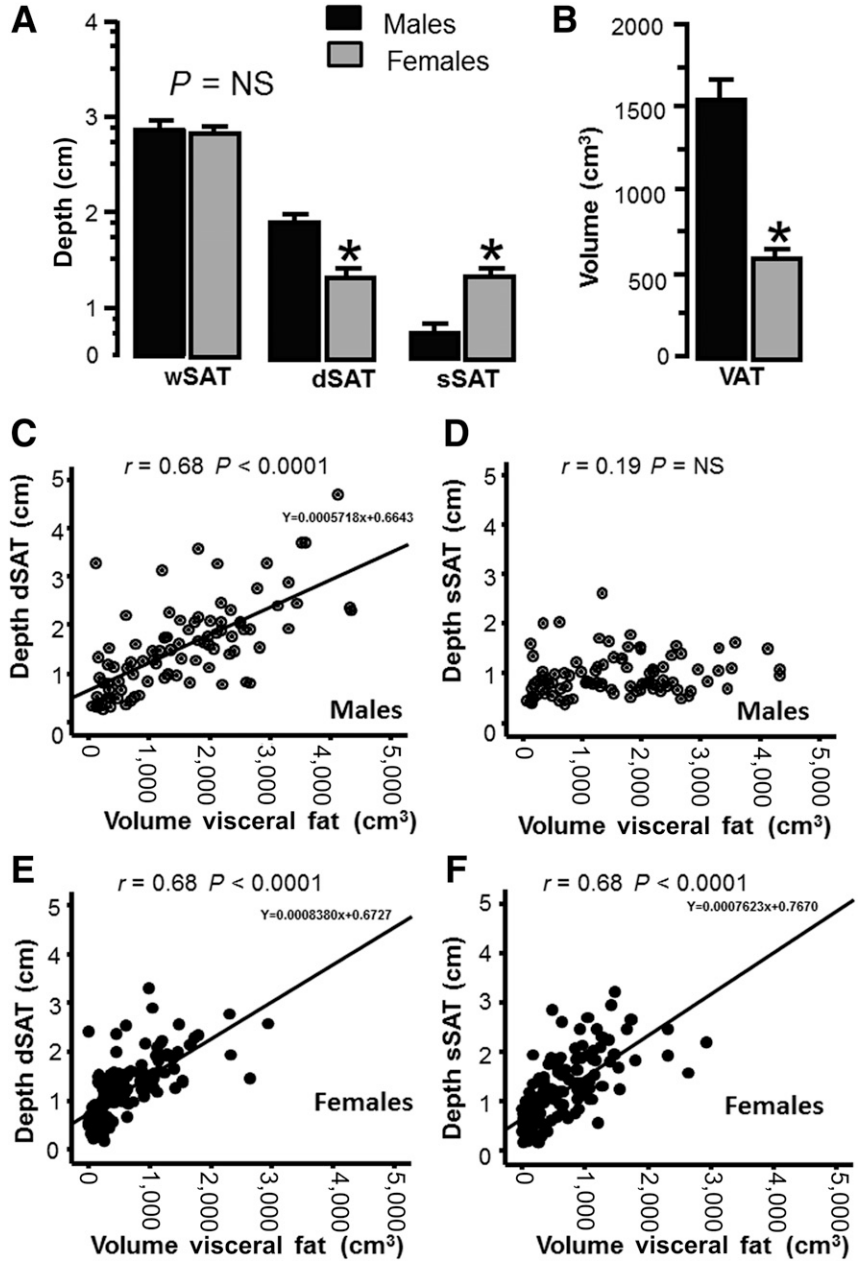

Figure 1—Comparison of whole subcutaneous fat (wSAT), deep subcutaneous fat (dSAT), superficial subcutaneous fat (sSAT), and VAT between males and females. *A* and *B*: Males had significantly greater dSAT and VAT but less sSAT than females (log-transformed values are expressed as mean ± SEM). Associations between VAT and sSAT/dSAT in males and females. In men, VAT was strongly associated with dSAT but not with sSAT (*C* and *D*), while in women, both SAT layers were similarly associated with VAT (*E* and *F*). *$P < 0.0001$ versus males.

dSAT Is Related to VAT in Men

In males, only dSAT was associated with VAT, while in females, both layers were associated with VAT (Fig. 1*C*–*F*).

mRNA Expression of Inflammatory, Lipogenic, and Lipolytic Target Genes in the SAT Layers

The expression of *ADIPOQ* was similar in the tissues from the two SAT layers, while the expression of *ADIPOR1* was higher (+19%; $P = 0.02$) in sSAT compared with dSAT. *LEP* (+35%; $P < 0.0001$), *LIPE* (+19%; $P = 0.03$), and *LPL* (+19%; $P = 0.02$) were all more highly expressed in dSAT compared with sSAT (Fig. 2). Genes involved in inflammatory pathways such as *IL6* (+21%; $P = 0.02$) and *MCP1* (+40%; $P = 0.02$) were also more highly expressed in the dSAT compared with sSAT. The dSAT layer

also showed higher expression of genes involved in FA synthesis (*FASN*, +18%, *P* = 0.003; *SCD1* +20%, *P* = 0.02; *ELOVL6*, +26%, *P* = 0.05) and adipogenic markers (*PPARγ2*, +20%, *P* = 0.003) (Fig. 2).Men displayed higher expression of genes involved in inflammatory pathways in dSAT (*IL6* +27%, *P* = 0.05; *MCP1* +25%, *P* = 0.006) compared with sSAT, higher *ADIPOR1* in sSAT versus dSAT (+30%; *P* = 0.05), higher *ADIPOR2* in dSAT versus sSAT (+12%; *P* = 0.03), and higher *LIPE* in dSAT versus sSAT (+19%; *P* = 0.02). Women expressed more *FASN* in dSAT versus sSAT (+7%; *P* = 0.02), and there was a trend for higher *ELOVL6* expression in dSAT versus sSAT (+20%; *P* = 0.054).

FA Composition of SAT Layers

As SAT layers are exposed to the same environment, one can make the assumption that any difference in TG FA composition depends on within-tissue metabolic differences (Table 1). Interestingly, dSAT, which had higher *FASN* mRNA expression compared with sSAT, also had higher relative quantities of the end products of FA synthesis (14:0 *P* = 0.029 and 16:0 *P* = 0.002). The proportion of 16:0 was also significant after normalizing to an exogenous FA that cannot be produced by the tissue; 18:2n-6 (*P* = 0.017). The immediate desaturation product of 16:0, 16:1n-7, was lower in dSAT compared with sSAT, despite the higher mRNA content of *SCD1*. The "desaturation index" (16:1n-7/16:0) was also lower in dSAT. However, within sSAT, there was a very strong correlation between the desaturation index and the mRNA content of *SCD1* (*r* = 0.78; *P* = 0.0001). It could be that the corresponding but weaker (*r* = 0.54; *P* = 0.009) association in dSAT was disrupted by the higher FA synthesis (generating larger quantities of the precursor). Both FA ratios indicative of fatty acyl elongation (18:0/16:0 and 18:1n-7/16:1n-7) were higher in dSAT compared with sSAT.

dSAT Has a Higher Proportion of Small Adipocytes Compared With sSAT

Examination of cell size distribution in the 23 paired biopsy specimens showed adipocyte size to be significantly different between sSAT and dSAT (Fig. 3). The dSAT layer had a greater proportion of small adipocytes (<500 μm^2) compared with sSAT (*P* = 0.015). Using the entire data set, there was a shift in adipocyte size distribution toward smaller adipocytes in the dSAT (Fig. 3*B*) and a trend toward larger median cell size in sSAT (1.217 ± 45 μm^2 sSAT vs. 1.098 ± 45 μm^2 dSAT; *P* = 0.07). We further examined if this relationship in cell size was dependent on overall adiposity by observing the differences in cell size in subjects classified according to BMI. In the nonobese group (BMI <30 kg/m^2), median cell size was higher in sSAT compared with dSAT, while no differences were observed in the obese group (BMI ≥30 kg/m^2) (Fig. 3*C*). There was an inverse association between median cell size in dSAT and mRNA expression of FA metabolic genes such as *FASN* and *SCD1* (*r* = −0.50, *P* = 0.021 for *FASN*; *r* = −0.42, *P* = 0.047 for *SCD1*).

CONCLUSIONS

We provide robust evidence that the dSAT and sSAT have different functional characteristics and associate differently to obesity-related complications. Importantly, dSAT is the strongest predictor of IR and FRS in men, independent of other obesity indices. In women, however, although dSAT is also related with IR and FRS, in multivariable analysis it does not offer additional predictive value for either of the two

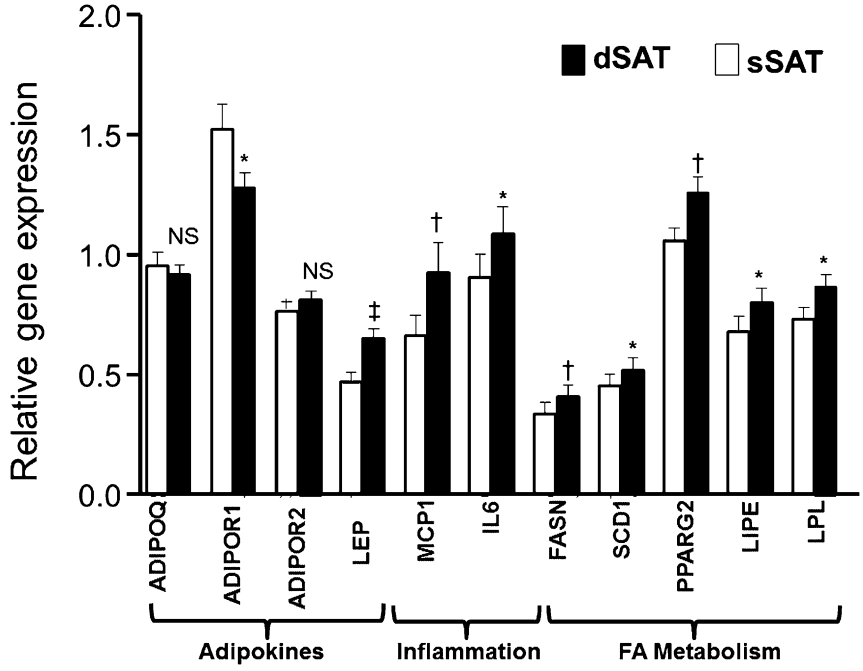

Figure 2—Differences in gene expression between sSAT and dSAT in 43 subjects (21 men and 22 women). Values expressed as mean ± SEM. *$P < 0.05$ versus males; †$P < 0.01$ versus males; ‡$P < 0.0001$ versus males. NS, not significant.

Table 1—FA composition of sSAT and dSAT

	sSAT	dSAT	*P* value
FA			
14:0	2.14 ± 0.10	2.53 ± 0.22	0.029
14:1 n-5	0.27 ± 0.04	0.22 ± 0.03	0.150
16:0	20.44 ± 0.43	21.06 ± 0.43	0.002
16:1 n-7	5.42 ± 0.31	4.51 ± 0.26	<0.001
18:0	3.08 ± 0.14	3.70 ± 0.16	<0.001
18:1 n-9	48.84 ± 0.53	48.84 ± 0.57	0.994
18:1 n-7	2.16 ± 0.04	2.14 ± 0.04	0.783
18:2 n-6	14.56 ± 0.40	13.87 ± 0.39	0.07
18:3 n-3	1.45 ± 0.09	1.44 ± 0.09	0.881
FA ratios			
16:1 n-7/16:0	0.27 ± 0.02	0.22 ± 0.01	<0.001
18:1 n-9/18:0	16.64 ± 0.82	13.79 ± 0.70	<0.001
18:0/16:0	0.15 ± 0.01	0.18 ± 0.01	<0.001
18:1 n-7/16:1 n-7	0.43 ± 0.03	0.51 ± 0.03	0.001
16:0/18:2 n-6	1.44 ± 0.06	1.55 ± 0.06	0.017

FA values are expressed as percentage of total FAs. Data are expressed as mean ± SEM. *n* = 22 for sSAT and dSAT.

readouts further to classical obesity indices such as BMI. The observations were obtained after developing and evaluating a new technique to assess the depth of the two layers using US. Adiposity in men is characterized by disproportionate expansion of dSAT compared with sSAT, and dSAT:wSAT ratio correlated more strongly to obesity-related complications in men than in women. It is also particularly strongly correlated with the VAT mass. Not only is it that the appreciation of distinct functional differences within the abdominal SAT layers appear to be gender specific and help explain the complex relationships between obesity and cardiovascular disease, but it also indicates that great care must be taken when accessing abdominal SAT for morphological or biochemical characterization.

Single-slice computed tomography and MRI have been used as tools to differentiate the SAT layers in small groups of individuals (10,13,14). The implementation and positive validation of US for the quantitative assessment of truncal SAT layers provides us with a new tool to make measurements more easily in larger numbers. The US technique is inexpensive and without any known health hazards and therefore useful in an epidemiological setting.

The relationship between VAT and IR is well-known, but few reports have investigated the relative contributions of SAT depots to metabolic traits (1,10,11,14,28–31).

Interestingly Miyazaki et al. (32) showed that VAT is associated with both peripheral and hepatic IR, independent of gender, in patients with type 2 diabetes but dSAT is associated with peripheral and hepatic IR in males, but not in females. In our study, greater thickness of the dSAT layer was strongly associated with both global and liver-specific IR in men. However, in female adiposity, the two layers were expanded similarly, and the qualitative difference between the fat layers may explain some of the differences in precipitation of IR between the genders.

Similar gender-specific differences were seen for the lipid markers related to cardiovascular disease. In men, statistically significant associations were only observed between dSAT and TG, apolipoprotein B, and apolipoprotein A1, whereas in women, dSAT and sSAT showed essentially the same significant associations with the CVR factors. Fasting glucose, which is one of the strongest predictors for diabetes risk, was only associated with dSAT in men, whereas similar significant associations between the layers were observed in women.

The tissue-specific effect of sex hormones on proliferation/differentiation of adipocytes and the expansion of specific AT depots in obesity (visceral in males and gluteal in females) are well described (33). Therefore the strong correlations between dSAT and VAT in our study imply that dSAT and VAT may be functionally similar, and they could have similar responses to sex hormones (being expanded in male adiposity leading to IR).

In within-subject paired biopsy samples, we observed that the median cell size was larger in sSAT compared with dSAT, while the cell size distribution was different between the two layers, with dSAT having higher abundance of the smallest adipocytes. McLaughlin et al. (34) have suggested that adipocytes within SAT from patients with IR are smaller and show higher expression of proinflammatory cytokines. Although it is not clear from those studies which fat layer was used, this concept fits well with our observations of higher cytokine expression in the dSAT, which is more closely associated with IR. We observed that in subjects with BMI <30 kg/m^2, sSAT adipocyte size is disproportionally increased compared with dSAT. In obese individuals (BMI ≥ 30 kg/m^2), the adipocyte cell size in dSAT is increased and in sSAT is decreased in a way that cell size in the two layers becomes equal, suggesting that the increased size of SAT in obesity and IR (35) could be largely attributable to increased cell size in the dSAT of these subjects.

The mechanistic background to this association is unclear, but it has been speculated that it depends on the inability of adipocytes to adequately respond to the increasing need for fat storage (34). Adipocytes in sSAT may have a greater ability for FA storage, and for this reason, the cells increase their size while recruitment of new adipocyte might be a feature of dSAT since *PPARγ2* expression levels are higher in dSAT than in sSAT. It is also possible that adipocytes from the two layers are fundamentally different, and the presence of smaller cells in dSAT is a reflection of an inability to significantly increase fat storage, leading to inflammation and stress signals observed here (34), while lack of adipocyte growth and impaired differentiation could be a form of

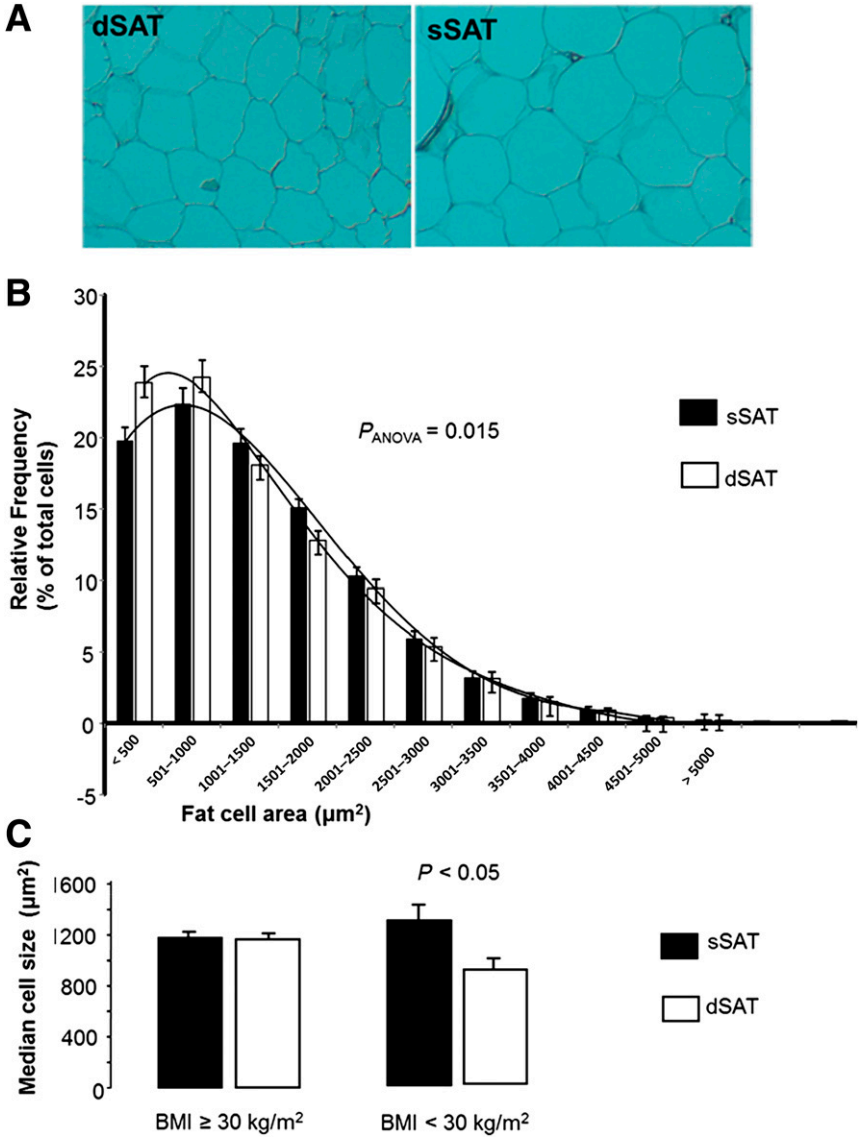

Figure 3—*A*: Sections of sSAT and dSAT. *B*: Frequency distribution of adipocyte cell surface area from dSAT and sSAT revealed an increased proportion of small adipocytes in the dSAT compared with the sSAT. *C*: Comparison of median adipocyte cell surface area from dSAT and sSAT. $n = 23$ per group; >100 cells were measured for each biopsy.

adiposopathy (acquired lipodystrophy) (36). Otherwise, it is the large adipocyte size that has been associated with IR (35), higher inflammatory profile (37), and diabetes risk (38). It is possible that these associations depend on the tissue studied, and even within the subcutaneous abdominal tissue, there are differences that can explain these paradoxical findings.

Previous investigations have demonstrated differential gene expression between SAT and VAT depots (7–9). Walker et al. (7) reported differences in gene expression (leptin, 11β-HSD1, resistin) between sSAT and dSAT obtained from 10 volunteers undergoing abdominal surgery. In the current study, we included males and females over a wide range of adiposity (BMI 17.9–46.2 kg/m^2) and found a higher expression of inflammatory genes (*MCP1*, *IL6*) in the dSAT compared with sSAT in men, but not in women. This finding is in general agreement with two earlier studies (8,9).

Adipocytes isolated from dSAT have been reported to have higher lipolytic activity compared with sSAT adipocytes (39). The higher expression of both *LIPE* and *LPL* that we found in dSAT compared with sSAT suggest that this tissue is metabolically more active. In addition, dSAT also showed higher expression of *FASN* and *SCD1*, and this was functionally supported by the TG FA composition of the tissue, where the dSAT had higher abundance of saturated FA (end products of de novo lipogenesis). Although the *SCD1* mRNA expression was higher in dSAT compared with sSAT, the marker for SCD1 activity (the desaturation index) was significantly higher in sSAT. This corresponded well with a similar and recent observation from our laboratory comparing the abdominal and gluteal tissue (40), where a higher abundance of

16:1n-7, a proposed insulin-sensitizing lipokine, was noted in gluteofemoral compared with abdominal AT. In the current study, the SAT layer with the weaker association to IR (sSAT) had the highest abundance of 16:1n-7.

Although the biology of abdominal dSAT appears to have similarities to VAT, the links we identify in this study between cardiometabolic risk and features in the expansion and biology of dSAT may not necessarily be causal. Dysfunction of peripheral (not only abdominal) AT may also play a role in the overall capacity for fat storage, and it is possible that because of impaired adipogenesis, peripheral AT depots may not be able to store excessive energy during positive caloric balance, resulting in energy overflow to other fat depots (such as dSAT, VAT, and even ectopic fat) (41). In this scenario, an increase in abdominal dSAT and VAT could be considered a surrogate biological manifestation of global AT dysfunction.

The descriptive nature of the study does not allow any final conclusions on the biological importance of our findings, and further mechanistic studies are required to explore the AT-specific functional differences between dSAT and sSAT.

Collectively, it is underpinned by clear functional differences between the two distinct fat layers in the abdominal wall that dSAT is the part of SAT that matters for the relationship to obesity-related complications, at least in men, and may have a different role than sSAT in the pathophysiology of male-pattern adiposity and subsequent risk of diabetes and cardiovascular disease.

Acknowledgments. The authors thank M. Gilbert, S. Humphreys, L. Dennis, S. Beatty, and J. Cheeseman (all University of Oxford) for their assistance.

Funding. This study was funded by the European Commission under the Marie Curie Programme (FP7-PEOPLE-2011-IEF). This study was also partly supported by the British Heart Foundation (project grants PG/09/003 and PG/12/78/29862). L.H. is a British Heart Foundation Intermediate Fellow in Basic Science.

Duality of Interest. No potential conflicts of interest relevant to this article were reported.

Author Contributions. K.M. and L.H. wrote the manuscript and conducted the experimental procedures. S.K.V., R.B., K.B., and M.K. edited the manuscript. B.A.F. wrote the manuscript. A.C. and M.J.N. conducted the experimental procedures. F.K. wrote the manuscript and designed and had the overall supervision of the study. F.K. is the guarantor of this work and, as such, had full access to all the data in the study and takes responsibility for the integrity of the data and the accuracy of the data analysis.

References

1. Smith SR, Lovejoy JC, Greenway F, et al. Contributions of total body fat, abdominal subcutaneous adipose tissue compartments, and visceral adipose tissue to the metabolic complications of obesity. Metabolism 2001;50:425–435
2. Després JP. Intra-abdominal obesity: an untreated risk factor for Type 2 diabetes and cardiovascular disease. J Endocrinol Invest 2006;29(Suppl.):77–82
3. Stefan N, Hennige AM, Staiger H, et al. High circulating retinol-binding protein 4 is associated with elevated liver fat but not with total, subcutaneous, visceral, or intramyocellular fat in humans. Diabetes Care 2007;30:1173–1178
4. Després JP, Lemieux I. Abdominal obesity and metabolic syndrome. Nature 2006;444:881–887
5. Johnson D, Dixon AK, Abrahams PH. The abdominal subcutaneous tissue: computed tomographic, magnetic resonance, and anatomical observations. Clin Anat 1996;9:19–24
6. Lancerotto L, Stecco C, Macchi V, Porzionato A, Stecco A, De Caro R. Layers of the abdominal wall: anatomical investigation of subcutaneous tissue and superficial fascia. Surg Radiol Anat 2011;33:835–842
7. Walker GE, Verti B, Marzullo P, et al. Deep subcutaneous adipose tissue: a distinct abdominal adipose depot. Obesity (Silver Spring) 2007;15:1933–1943
8. Tordjman J, Divoux A, Prifti E, et al. Structural and inflammatory heterogeneity in subcutaneous adipose tissue: relation with liver histopathology in morbid obesity. J Hepatol 2012;56:1152–1158
9. Alvehus M, Burén J, Sjöström M, Goedecke J, Olsson T. The human visceral fat depot has a unique inflammatory profile. Obesity (Silver Spring) 2010;18:879–883
10. Kelley DE, Thaete FL, Troost F, Huwe T, Goodpaster BH. Subdivisions of subcutaneous abdominal adipose tissue and insulin resistance. Am J Physiol Endocrinol Metab 2000;278:E941–E948
11. Golan R, Shelef I, Rudich A, et al. Abdominal superficial subcutaneous fat: a putative distinct protective fat subdepot in type 2 diabetes. Diabetes Care 2012;35:640–647
12. Johnson D, Cormack GC, Abrahams PH, Dixon AK. Computed tomographic observations on subcutaneous fat: implications for liposuction. Plast Reconstr Surg 1996;97:387–396
13. Kohli S, Sniderman AD, Tchernof A, Lear SA. Ethnic-specific differences in abdominal subcutaneous adipose tissue compartments. Obesity (Silver Spring) 2010;18:2177–2183
14. Misra A, Garg A, Abate N, Peshock RM, Stray-Gundersen J, Grundy SM. Relationship of anterior and posterior subcutaneous abdominal fat to insulin sensitivity in nondiabetic men. Obes Res 1997;5:93–99
15. Mersmann HJ, Leymaster KA. Differential deposition and utilization of backfat layers in swine. Growth 1984;48:321–330
16. Tan GD, Goossens GH, Humphreys SM, Vidal H, Karpe F. Upper and lower body adipose tissue function: a direct comparison of fat mobilization in humans. Obes Res 2004;12:114–118
17. Chandalia M, Lin P, Seenivasan T, et al. Insulin resistance and body fat distribution in South Asian men compared to Caucasian men. PLoS ONE 2007;2:e812
18. Manolopoulos KN, Karpe F, Frayn KN. Gluteofemoral body fat as a determinant of metabolic health. Int J Obes (Lond) 2010;34:949–959
19. Tan GD, Neville MJ, Liverani E, et al. The in vivo effects of the Pro12Ala PPARgamma2 polymorphism on adipose tissue NEFA metabolism: the first use of the Oxford Biobank. Diabetologia 2006;49:158–168
20. Kaul S, Rothney MP, Peters DM, et al. Dual-energy X-ray absorptiometry for quantification of visceral fat. Obesity (Silver Spring) 2012;20:1313–1318
21. Matthews DR, Hosker JP, Rudenski AS, Naylor BA, Treacher DF, Turner RC. Homeostasis model assessment: insulin resistance and beta-cell function from fasting plasma glucose and insulin concentrations in man. Diabetologia 1985;28:412–419
22. Kotronen A, Lewitt M, Hall K, Brismar K, Yki-Järvinen H. Insulin-like growth factor binding protein 1 as a novel specific marker of hepatic insulin sensitivity. J Clin Endocrinol Metab 2008;93:4867–4872
23. Póvoa G, Roovete A, Hall K. Cross-reaction of serum somatomedin-binding protein in a radioimmunoassay developed for somatomedin-binding protein isolated from human amniotic fluid. Acta Endocrinol (Copenh) 1984;107:563–570
24. Neville MJ, Collins JM, Gloyn AL, McCarthy MI, Karpe F. Comprehensive human adipose tissue mRNA and microRNA endogenous control selection for quantitative real-time-PCR normalization. Obesity (Silver Spring) 2011;19:888–892
25. Hodson L, Neville M, Chong MF, et al. Micro-techniques for analysis of human

adipose tissue fatty acid composition in dietary studies. Nutr Metab Cardiovasc Dis 2013;23:1128–1133

26. Roberts R, Hodson L, Dennis AL, et al. Markers of de novo lipogenesis in adipose tissue: associations with small adipocytes and insulin sensitivity in humans. Diabetologia 2009;52:882–890
27. Chen HC, Farese RV Jr. Determination of adipocyte size by computer image analysis. J Lipid Res 2002;43:986–989
28. Abate N, Garg A, Peshock RM, Stray-Gundersen J, Adams-Huet B, Grundy SM. Relationship of generalized and regional adiposity to insulin sensitivity in men with NIDDM. Diabetes 1996;45:1684–1693
29. Abate N, Garg A, Peshock RM, Stray-Gundersen J, Grundy SM. Relationships of generalized and regional adiposity to insulin sensitivity in men. J Clin Invest 1995; 96:88–98
30. Goodpaster BH, Thaete FL, Simoneau JA, Kelley DE. Subcutaneous abdominal fat and thigh muscle composition predict insulin sensitivity independently of visceral fat. Diabetes 1997;46:1579–1585
31. Koska J, Stefan N, Votruba SB, Smith SR, Krakoff J, Bunt JC. Distribution of subcutaneous fat predicts insulin action in obesity in sex-specific manner. Obesity (Silver Spring) 2008;16:2003–2009
32. Miyazaki Y, Glass L, Triplitt C, et al. Abdominal fat distribution and peripheral and hepatic insulin resistance in type 2 diabetes mellitus. Am J Physiol Endocrinol Metab 2002;283:E1135–E1143
33. Mayes JS, Watson GH. Direct effects of sex steroid hormones on adipose tissues and obesity. Obes Rev 2004;5:197–216
34. McLaughlin T, Sherman A, Tsao P, et al. Enhanced proportion of small adipose cells in insulin-resistant vs insulin-sensitive obese individuals implicates impaired adipogenesis. Diabetologia 2007;50:1707–1715
35. Lundgren M, Svensson M, Lindmark S, Renström F, Ruge T, Eriksson JW. Fat cell enlargement is an independent marker of insulin resistance and 'hyperleptinaemia'. Diabetologia 2007;50:625–633
36. Bays HE, González-Campoy JM, Bray GA, et al. Pathogenic potential of adipose tissue and metabolic consequences of adipocyte hypertrophy and increased visceral adiposity. Expert Rev Cardiovasc Ther 2008; 6:343–368
37. Skurk T, Alberti-Huber C, Herder C, Hauner H. Relationship between adipocyte size and adipokine expression and secretion. J Clin Endocrinol Metab 2007;92:1023–1033
38. Yang J, Eliasson B, Smith U, Cushman SW, Sherman AS. The size of large adipose cells is a predictor of insulin resistance in first-degree relatives of type 2 diabetic patients. Obesity (Silver Spring) 2012;20: 932–938
39. Monzon JR, Basile R, Heneghan S, Udupi V, Green A. Lipolysis in adipocytes isolated from deep and superficial subcutaneous adipose tissue. Obes Res 2002;10:266–269
40. Pinnick KE, Neville MJ, Fielding BA, Frayn KN, Karpe F, Hodson L. Gluteofemoral adipose tissue plays a major role in production of the lipokine palmitoleate in humans. Diabetes 2012;61:1399–1403
41. McQuaid SE, Hodson L, Neville MJ, et al. Downregulation of adipose tissue fatty acid trafficking in obesity: a driver for ectopic fat deposition? Diabetes 2011;60:47–55